Towards A Mid-Latitude Ocean Frequency-Wavenumber Spectral Density and Trend Determination

Carl Wunsch

Department of Earth, Atmospheric and Planetary Sciences

Massachusetts Institute of Technology

Cambridge MA 02139 USA

email: cwunsch@mit.edu

March 18, 2010

Abstract

The time- and space-scale descriptive power of two-dimensional Fourier analysis is exploited to re-analyze the behavior of mid-latitude variability as seen in altimetric data. These data are used to construct a purely empirical, analytical, frequency-zonal wavenumber spectrum of ocean variability for periods between about 20 days and 15 years, and on spatial scales of about 200km to 10000km. The spectrum is dominated by motions along a "non-dispersive" line which is a robust feature of the data, but for whose prominence a complete theoretical explanation is not available. The estimated spectrum also contains significant energy at all frequencies and wavenumbers in this range, including eastward-propagating motions, and which are likely some combination of non-linear spectral cascades, wave propagation, and wind-forced motions. The spectrum can be used to calculate statistical expectations of spatial average sea level, and transport variations. But because the statistics of trend-determination in quantities such as sea level and volume transports depend directly upon the spectral limit of the frequency approaching zero, the appropriate significance calculations remain beyond reach—as low frequency variability is indistinguishable from trends already present in the data.

1 Introduction

Attention to oceanic variability has tended to focus on two particular, if disparate, phenomena: (1) the intense mesoscale eddy field with nominal timescales of months and spatial scales (here defined as wavelengths) of hundreds of kilometers[1] and, (2) long period trends of decadal and longer time durations and (usually) of basin to global scale.

Zang and Wunsch (2001, hereafter ZW2001) attempted a partial synthesis of variability that was, because of the available data, largely confined to (1) and in the northern hemisphere. Discussions of phenomenon (2) have tended to focus on multi-decadal heat and salt content changes as determined from hydrography (see the summary in Bindoff et al., 2007), and the related shifts in sea level (e.g., Cazenave and Nerem, 2004). Despite the disparities of time and space scales, it is not ultimately possible, for a number of reasons, to discuss these changes separately. Of fundamental importance, one requires an accurate estimate of the nature of the background variability before significance levels can be assigned to any apparent trend. Furthermore, as climate models begin to resolve the eddy field, the question of whether they are doing so realistically in terms of basic statistics of frequency and wavenumber will loom very large. Apart from some ad hoc studies, it is difficult to describe the behavior of ocean variability between about one cycle/year and the longest periods of interest—where apparent trends are displayed. In particular, the spectral structure for length scales longer than a few hundred kilometers, on time scales exceeding a few months is essentially unknown.

In a purely formal sense, the problem of determining the significance of apparent trends in one-dimensional stochastic data reduces to that of characterizing the behavior of the

[1]The dominant eddy field corresponds to the atmospheric synoptic scale, not the mesoscale, but it is too late to change the label.

frequency power density, $\Phi_s(s)$ in the limit as $s \to 0$. Smith (1993), Beran (1994), Overland et al. (2006), Vyushin and Kushner (2009) and others have discussed "long-memory" processes in which the behavior for small s is sufficiently "red" that the temporal covariances decay algebraically rather than exponentially as in more conventional processes. This behavior greatly reduces the number of degrees-of-freedom in trend estimation and its existence would be very troubling for climate change detection. The word "formal" is thus used here—because in practice the behavior at the limit is both unknown and indeterminate; all real records being of finite duration, no physical system exists for infinite time. As durations increase, the characterization of real records as either stochastic or deterministic also ceases to have meaning. At best, one can try to characterize a system over time scales for which observations exist and to understand the implications should that behavior continue to be appropriate as arbitrarily longer time scales are addressed.

In this paper some of these issues are made concrete by taking a small step toward deducing the behavior of *some* elements of the ocean circulation using altimetric and tide gauge records as the primary vehicle so as to frame the discussion that needs to take place for understanding trends. The altimetric record is the present focus because it is the only one in existence exceeding a decade in length that is also continuous, near-global and, through its role as the surface pressure, representative of large-scale interior dynamics. At least three ways to use these data exist: the raw, along-track observations (see Fu and Cazenave, 2000 for a general description of altimeter data), the sea surface height (SSH) derived from a GCM constrained through least-squares to the raw along-track data (as in Wunsch and Heimbach, 2007); and the altimetric data as gridded through the TOPEX/-POSEIDON—Jason projects (Le Traon et al., 1998). The effects of gridding are not negligible, but are also not of zero-order importance here, and so for convenience, we use that product.

In practice, as will be seen, discussion reduces to understanding the frequency-wavenumber character of oceanic variability. Because the climate system has an endless array of memory time scales—in the ocean, seconds to 10,000 years; in the land glaciers, days to 100,000 years; and in the biota (albedo, etc.) arbitrarily long time scales—the instrumental record of change can hardly be expected to depict more than a minuscule fragment of the ongoing temporal changes, and whose "long-memory" may be completely conventional.

2 The North Pacific

2.1 Basic Description of Altimetric Data

The latitude band (see chart in Fig. 1) 20°N to 40.75°N spanning the width of the Pacific Ocean is used to establish the basic ideas. The analysis uses the 7-day average gridded product provided by the AVISO project (as described by Le Traon, et al., 1998) but which, as it is heavily manipulated, should not be confused with the raw data. In particular, spatial scales below about 300km have been suppressed by the gridding procedure. This region was chosen arbitrarily as likely being typical of subtropical gyres (see Zang and Wunsch, 1999). Fig. 2 shows four weekly estimates of the topographic anomaly in the gridded data set. That there is strong persistence from week-to-week with subtle changes between weeks, is evident.

Fig. 3 shows the logarithm of net temporal variance as a function of position. The three-order of magnitude spatial non-stationarity in the variance renders very incomplete any simple spectral description of its behavior. (Such a description is still valid, but unlike the case for spatially and temporally stationary fields, the ordinary spectral density is only the first term in an infinite series of higher-order spectral moments required for a complete representation.)

Sea surface height variability at any given point (here representing small regions of approximately 300km diameter as a result of the mapping algorithm), and the areal average have a distinct flavor. In what follows, the annual cycle has been left present as it is here quite weak, and has been much studied (e.g., Vinogradov et al., 2008).

The spatial structure of the trends are shown in Fig. 4 and which also shows some of the difficulties. The largest values exceed 30cm/y, but most are smaller than 10cm/y. On average, the trend here is positive, but it is clearly a small residual of positive and negative changes (this region is that of the Kuroshio extension, and on the west is one of the noisiest parts of the ocean). Estimates of the near-global trends can be seen in Cazenave and Nerem (2004) and Wunsch et al. (2007) among others.

3 Periods to 15 years

Consider the $k-s$ (circular wavenumber and frequency) power density estimate, $\Phi(k,s)$ of surface elevation, η, shown in Fig. 5 from altimetric data (Wunsch, 2009) in the eastern region of the North Pacific box (a similar set of results from the South Pacific Ocean can be seen in Maharaj et al., 2007). Its integrals are the frequency, and wavenumber spectra,

$$\Phi_k(k) = \int_0^{s_{\max}} \Phi(k,s)\,ds, \quad \Phi_s(s) = \int_{-k_{\max}}^{k_{\max}} \Phi(k,s)\,dk, \tag{1}$$

where the limits are determined by the sampling properties of the gridded values, and are shown in Fig. 6. These diagrams were described by Wunsch (2009). Here, note particularly that much of the energy lies along the "non-dispersive" line in wavenumber-frequency space. Chelton et al. (2007) and many other authors have focussed on these motions. A significant fraction of the energy exists, however, at large distances from this line, including that of eastward-going motions (20% of the total is eastward-going, 70% westward, and 9% indistinguishable from standing wave energy). The non-dispersive line is nearly tangent to the first baroclinic mode dispersion curve (shown in the figure) near zero k, s and intersects the barotropic dispersion curve at large k, s. This behavior appears to be typical of much of the ocean, but with high latitudes, including the Southern Ocean, being distinctly different (not shown here).

An estimate of the corresponding meridional wavenumber-frequency spectrum is shown in Wunsch (2009), with a predominance of long meridional scale energy and is not further considered here. (Glazman et al., 2005 discuss the general topic, but their results are not typical of this region.) Suggestions exist that zonal jet-like features are important in the ocean circulation (e.g., Maximenko et al., 2008 and references there), but if present in the altimetry at this location, they are, relatively, very weak in the time-dependent components. (Geoid accuracy is insufficient on those scales to discuss the time-mean.)

It is not the intention in this paper to produce a global discussion, but to provide a framework for it. Fig. 7 displays the logarithmic frequency-zonal wavenumber spectrum for the considerably higher latitude of 41°N—the northern edge of the study box. A residual of the nondispersive line is visible, lying along a much less steep straight line. Consistent with inferences of Tulloch et al. (2009), the dominance of the excess energy energy along the nondispersive line is reduced, with a corresponding relative increase in the energy of the eastward-going motions, and much energy close to $k = 0$. At the northern edge of the box, the relative energies are nearly equally divided between eastward- and westward-going motions, and the ZW2001 representation becomes more accurate.

A reviewer of this paper insists that adequate theory exists to explain the structure of Fig. 5, and thus we briefly digress to summarize some of the issues, which are treated at greater length by Ferrari and Wunsch (2010; hereafter FW2010, and in Vallis, 2006, etc.). Beginning with Chelton and Schlax (1996), the published focus has been on the apparent phase velocity of altimetric disturbances, often determined through a Radon transform. This approach calculates straight-line integrals through the longitude-time fields, seeking the maximum value corresponding to the dominant phase velocity. It lumps together all wavenumbers irrespective of frequency, and thus isolates the existence of the non-dispersive line as the dominating feature of the data at mid- and low-latitudes.

Theoretical explanations for the makeup and structure of the overall wavenumber, and frequency-wavenumber, spectra fall into a small number of categories: (1) Wave theories, in which the motions are dominantly free, with a physics ranging from the "basic textbook theory" (BTT) of a flat-bottom, linear, resting, etc., ocean, to their modification by variable background flows, stratification, topography, etc. (2) Instability theories, where the variability results from the breakdown of mean currents and is described by waves with properties of the most unstable modes, but overlapping the physics contained in (1). (3) Forced wave theories, encompassing both stable and unstable background flows. As wave theories, (1-3) can produce dispersion relationships between k (and/or l) and s, although in the forced case, the $k-s$ space is filled out by the imposed forcing spectrum subject to full or near-resonant amplifications. (4) Turbulence theories result in a fully disordered field, with no dispersion relationship available. The ultimate energy sources can be either or both of forced or unstable motions. Theory predicts only the $k-$spectra, but Eulerian frequency spectra can sometimes be inferred through Taylor's hypothesis, $k = Us$, where U is either a large-scale advective flow or an RMS velocity of the energy containing eddies. Further theory predicts the emergence of wave physics at meridional scales larger than the Rhines (1977) $L_R \propto (U/\beta)^{1/2}$, because turbulence is arrested at those scales (β is the conventional meridional derivative of the Coriolis parameter). These elements overlap and interact. For example, Isachsen et al. (2007) show how instability of the waves in (1) can drive energy away from any dispersion curve.

A full review of these various theories and their relationship to the empirical spectra would require much more space than is available here. Suffice it to say that the predominant motions present do not have an obvious relationship to (1) except at the very lowest observable frequencies where they are indistinguishable from the linear dispersion curves. Both the Taylor hypothesis and turbulent flows subject to $\beta-$effects involve parameters usually labelled U. Taylor originally defined U as a large-scale mean velocity advecting isotropic turbulence past fixed sensors (see e.g., Hinze, 1975) although it has been reinterpreted in the Rhines (1977) sense as an eddy RMS. In the present case, it is difficult to see why, in either case, U should have a latitudinal dependence producing the non-dispersive line slope of βR_d^2 or how the RMS advecting flow could be so remarkably stable that the slope is maintained so sharply for 16 years. None of the spectra examined here show a wavenumber gap permitting an easy selection of the transition between energy- and enstrophy-dominant scales, nor to my knowledge, does the theory permit an explicit calculation of the structure seen in Fig. 5. FW2010 concluded that forced motions describe a significant fraction of the observed motions not on the nondispersive line—but not necessarily a majority of it.

Included in (1) is the literature rationalizing the "too-fast" phase velocity first pointed out by Chelton and Schlax (1996). Maharaj et al. (2007) show that the mean potential vorticity theory of Killworth and Blundell (2003b) describes much of the motion along the low frequency end of the nondispersive line in the South Pacific, but not the energy located elsewhere in $s-k$ space. Again, why the nondispersive line should emerge with the slope, βR_d^2, noted above, is not so clear. Alternative hypotheses also exist, particularly those related to the influence of bottom topography (Tailleux and McWilliams, 2001; Killworth and Blundell, 2003a), whose tendency to reduce the abyssal velocities can produce coupled modes with faster phase velocities. This latter mechanism will be touched on later, as it has testable consequences for mooring data.

Behavior of U

The existence of the variable U in the turbulence theories suggests the utility of a brief examination of the temporal and spatial structure of the large scale flows. Consider, as an example, the large-scale flow field in the boxed region as inferred from the so-called ECCO-GODAE solution v3.73 discussed by Wunsch and Heimbach (2009). This estimate, based upon a 1° horizontal resolution GCM, represents a least-squares fit to a very large data set coincident with the altimetric record used here, including not only the altimetry, but also hydrography, etc. No eddies are present with this resolution, and in the open ocean, the resulting time-varying estimate can be thought of as a field in thermal wind balance, within error bars, of all of the data, thus reflecting the gradients on sub-basin and larger scales. To keep the discussion from proliferating unduly, we use the vertical water-column average monthly mean zonal flows, setting aside the difficult question of the vertical structure of U. This choice is made because, as discussed below, current meter mooring data are interpreted here as implying a linear low mode (the barotropic and lowest baroclinic modes) structure—one which could not be maintained in a strongly sheared, time-varying, background flow. Hypotheses depending upon the depth of integration could be explored, but are not taken up here.

The latitude range was restricted to 27.5°N to 31.5°N. Fig. 8 shows the monthly mean U and its spatial standard deviation over the strip, as well as the time average of U showing the spatial structure. In general, the time average $U << \beta R_2^2$, the approximate slope of the nondispersive line, but its variability is sufficiently great that it could broaden the dispersion curve. Kinetic energy in the ocean is 95-99% bound up in the variability (e.g., Ferrari and Wunsch, 2009). All this simply says that the ocean appears noisy out to the longest records that we have, and that any separation between large- and meso-scales is an arbitrary one—precluding a simple estimate of U in any of its definitions.[2]

An Analytical Curve Fit

Can one find an analytical form sufficiently accurate to use in calculating temperature or transport variations and trends? Among the many possibilities, are the one the same referee insists is the "correct" one,

$$\Phi(k,s) = \frac{A(\phi,\lambda)}{\left(s + k\beta R_d^2\right)^2 + a_1^2} \tag{2}$$

where a_1 is a constant, and which emerges from the linear damped-resonance model e.g., of Frankignoul et al. (1997). This form was one of the first tried (not shown), but was rejected because it gave a poor fit, both in not exhibiting the narrowness and large amplitude of the non-dispersive line energy, but also because it failed to adequately describe the significant amounts of energy lying far from that line. Consider, instead, as

[2] One might argue that U should be determined by the eddy field that has been suppressed here by use of a 1° horizontal resolution model. But eddy-permitting models (e.g., Mazloff et al., 2010) show no recognizeable dividing point between the eddy field and larger scale flow, and no such model has yet been run constrained to be consistent with the global data sets. In any event, it is not so easy to test such models for realism. Any field, $\tilde{U}$, derived from the eddy field will show a stochastic behavior that would need to be tested.

a starting point,

$$\Phi\left(k,s\right)=A\left(\phi,\lambda\right)\left\{\mathrm{sech}^4\left(\frac{\beta R_d^2 k+s}{0.008}\right)\exp(-\left(100s\right)^2)+\frac{0.01}{a_1+a_4k^4+\delta_1 s^2}\right\}, \quad (3)$$

{phiks1}

$$0\leq s\leq 1/7d,\ -1/100\leq k\leq 1/100\mathrm{km}$$

$$\beta R_d^2=4\mathrm{km/d},\ a_4=\left(200\mathrm{km}\right)^4,\ a_1=0.01,\quad \delta_1=\left(14\mathrm{day}\right)^2.$$

where the sech^4 produces the excess energy along the non-dispersive line in Fig. 5 and the second term accounts for the broad continuum away from that line. The sech^4 term was introduced to represent the exponential decline in energy away from the non-dispersive line. The only physically-based parameter is βR_d^2, and a crude accounting for latitudinal changes within the subtropics can be obtained by permitting $\beta\left(\phi\right)R_d\left(\phi,\lambda\right)^2$ to be a slowly-varying function of position (latitude, ϕ, and longitude λ). $A\left(\phi,\lambda\right)$ is intended to be a slowly changing function of position, as in the ZW2001 energy amplitude factor. Fig. 9 shows how βR_d^2 varies with position, primarily with β. At high latitudes, the maximum phase velocities are so slow that linear physics are unlikely to apply. (Note 1km/day$\approx$ 1cm/sec.)

This form represents the non-dispersive motions as additive to a background continuum. The result is purely empirical and no claim is made that is "correct"—merely that it provides a reasonably efficient description of the estimated spectrum. Fig. 10 shows that the analytic form does do a reasonable job. In comparison to $\Phi_k\left(k\right)$, the form produces relatively too much eastward-going motion and an inadequate roll-off in wavenumber. It is important to keep in mind, however, that the high wavenumber behavior, beyond about 1/200km, of the altimetric data is essentially unknown. The high frequency limit $s_m=1/14$d corresponds to the 7-day gridding interval AVISO product. Note that the Garrett and Munk (1972) internal wave spectrum contains energy at 100km and shorter, and there is as yet no way of separating internal wave energy from that of the geostrophically balanced flows (see, in particular, Katz, 1975). The conspicuous appearance of internal tides in altimetric data shows emphatically that internal waves more generally will be present in altimetric data. A full oceanic frequency-wavenumber spectrum eventually must reflect the contribution from internal waves, balanced motions, and other ageostrophic energy. Because of the very large spatial variation in oceanic kinetic energies, A is chosen to impose,

$$\iint_{-\infty}^{\infty} \Phi\left(k, s\right) dkds = 1,$$

approximately, so that a local altimetric variance can be introduced as a multiplier to produce any regional energy level. As $s \to 0$, both $\Phi\left(k, s\right)$ and $\Phi_s\left(s\right)$ are independent of s, rendering the frequency spectrum as white noise. That inference is re-examined below.

As compared to ZW2001 and as used in Wunsch (2008), the form in Eq. (3) is nonseparable in k, s and which leads to greater analytical difficulties. A multitude of motions are being depicted, including free modes, meteorologically-forced motions reflecting atmospheric structures, the end products of turbulent cascades, ageostrophic motions having a surface expression, advection of near-frozen features, and instrumental noise, all superposed and sometimes interacting. A marginally better fit is obtained by retaining terms in k, k^2, etc., but they are probably not now worth the extra complexity.

The term in $\beta R_d^2 k + s$ reflects the inference that the non-dispersive line is approximately tangent to the first mode baroclinic Rossby wave dispersion curve as $k, s \to 0$ (see Wunsch, 2009) and which is suggested by the way the slope changes with latitude (Fig. 9). In practice, at best, one can say only that the tangency is not inconsistent with the data, albeit the estimated values of R_d are necessarily noisy, and the utility of a resting ocean hypothesis is doubtful for small s.

Both the estimate in Fig. 5 and the analytic expression Eq. (3) contain a great deal of structure implying that a choice of the various constants in the analytic expression will produce varying accuracies over the $k-s$ plane. At this stage, it is not completely clear what the most significant elements are. To proceed, note (e.g., Vanmarcke, 1983) that many of the physically important properties of a Gaussian random field depend only upon the spectral moments. Thus define,

$$\langle s^q \rangle = \int_0^{s_m} s^q \Phi_s(s)\, ds / \int_0^{s_m} \Phi_s(s)\, ds,$$
$$\langle k_w^q \rangle = \int_0^{k_m} k^q \Phi_k(k)\, dk / \int_0^{k_m} \Phi_k(k)\, dk, \quad \langle k_e^q \rangle = \int_{-k_m}^{0} k^q \Phi_k(k)\, dk / \int_{-k_m}^{0} \Phi_k(k)\, dk$$

where q is an integer. From the data, $1/\langle s \rangle = 164\text{d}$, $1/\sqrt{\langle s^2 \rangle} = 121\text{d}$, $1/\langle k_w \rangle = 696\text{km}$, $1/\sqrt{\langle k_w^2 \rangle} = 579\text{km}$, $1/\langle k_e \rangle = 1710\text{km}$, $-1/\sqrt{\langle k_e^2 \rangle} = -1/905\text{km}$. These values are independent of A. That the westward-going moments have shorter wavelengths than the eastward-going ones is consistent with the excess energy along the non-dispersive line. It remains to choose the constants in Eq. (3) to approximately reproduce these moments and are what led to the choice in Eq. (3). In comparison, the values obtained are, 177d, 138d, 573km, 471km, 1128km, 899km which are considered sufficiently close to the empirical ones to proceed (a formal fitting procedure could be employed). These values conveniently characterize the space and time scales of the variability, albeit with much loss of detail.

As the frequency tends toward 1/15years, the asymptotic spectral values are not trustworthy. Among other reasons, any trend present in the data will influence the spectral shape (see Appendix A for a brief discussion of the trend fitting problem). The spatial structure of the trends shown in Fig. 4 demonstrates some of the difficulties.

In the BTB theory (Longuet-Higgins, 1965), the highest frequency possible in a linear, first-mode Rossby wave is $s = \beta R_1/4\pi$ and which diminishes rapidly with latitude. The slope of the dispersion curve (the group velocity) as $s \to 0$, diminishes as βR_1^2. Thus as the latitude increases, the domain of the first mode Rossby wave becomes very small, higher modes having yet longer periods, and the linear, free-wave dynamics is decreasingly relevant (see Fig. 11). A high latitude theory is thus potentially, in one respect, simpler than a mid-latitude one, in eliminating the wave mechanisms present in the physical process list above.

3.1 The Low Frequencies and Wave Numbers

We now turn specifically to the spectral behavior with frequency and the behavior at periods longer than are accessible from the altimetric record. Mitchell (1976), Kutzbach (1978), Huybers and Curry (2006) and others have provided discussions of the spectrum of climate extending back into the remote past in a subject notable for its extremely scarce data.

As a guide, we start with the 103-year record available from the Honolulu, Hawaii tide gauge record (latitude 21.3°N just to the south of the altimetric box; taken from the website of the Permanent Service for Mean Sea Level, Liverpool), plotted in Fig. 12. This record is discussed in detail by Colosi and Munk (2006) and while the presence of the Hawaiian island arc raises questions about its representativeness of the open ocean, it at least provides an example of the problems faced in describing low frequency behavior of the sea surface height at time scales much longer than obtainable from the altimetric duration. Fig. 12 shows the spectral density estimate of the record calculated in two distinct ways, both for the original and detrended (trend of 1.5 ± 0.05mm/y) records.[3] The first method is based on a Daniell-window smoothed periodogram, and the second is the multitaper method (see e.g., Percival and Walden, 1993). Because the multitaper method is biassed at low frequencies (McCoy et al. 1998), the periodogram method provides the better estimates for small s. The major issue concerns the conventional trend removal and which in all cases shown converts the somewhat red spectrum at low frequencies into one that is reasonably described as white noise. Is the trend the secular one reflective of the extended deglaciation discussed below, or is it another low frequency fluctuation which will ultimately reverse, or is it an artifact of changing observational technologies and instrument positions? For present purposes, we explicitly assume that the trend is truly secular—defined as extending far beyond the record length, and will take as a starting point the assumption that at periods beyond about five years period, that the spectral density of sea surface height is white noise. (Sturges and Hong, 1995, suggested a drop in the spectral density at Bermuda for periods longer than about 8 years, but they were extrapolating beyond the region of conventional spectral estimation.)

The issue of the asymptotic value, $s \to 0$, of the spectrum is difficult. Huybers and Curry (2006) patched together various proxy data that can at least crudely be interpreted as large-regional scale temperatures extending back beyond 100,000 years. If taken literally (proxy records are not simple to interpret), a power law slope $s^{-1/2}$ would be representative out to about 100 years period, becoming much steeper than that at longer periods to about 100,000 years (where there is an energy excess). Their proxy spectra

[3] The standard error is based upon the assumption of a white noise background and is thus optimistic. That the trend is best regarded as a straight line is an assumption—one that is discussed further in Appendix A.

appear to flatten beyond 100,000 years, rendering the energy in the physical process as finite. But on the very longest time scales imaginable (giga-years), one has the formation of the ocean, which is not obviously stochastic. Evidently, very different physical regimes exist as time scales change, and any attempt to infer the limiting behavior $s \to 0$ will fail with a finite record length.

What do such results imply for the ocean? Assume that the Huybers and Curry (2006) results nominally represent atmospheric temperatures, T_a. In one of the simplest of all possible models, oceanic temperatures might depend upon the atmospheric ones through a rule,

$$\rho c_p V \frac{\partial T}{\partial t} = \gamma \left(T_a - T\right), \tag{5}$$

where γ is some constant and c_p is the oceanic heat capacity and V some relevant volume. Then the power density of ocean temperature is related to that of T_a (denoted Φ_a) as

$$\Phi\left(s\right) = \frac{\gamma'^2 \Phi_a\left(s\right)}{s^2 + \gamma'^2}, \quad \gamma' = \gamma/\rho c_p V \tag{6}$$

{airseaheat}

If $\gamma' >> s$, $\Phi\left(s\right) \propto \Phi_a\left(s\right)$ and will have the same power law. On the other hand if $\gamma' << s$, $\Phi\left(s\right) \propto \Phi_a\left(s\right)/s^{-2}$ and will be much steeper. A choice of γ is crucial. In modern ocean models, the time scales for ocean surface temperatures to be "nudged" toward atmospheric ones range from a few days to a month or so (see e.g., Frankignoul et al., 1998) and thus $s^2 << \gamma'^2$, and $\Phi\left(s\right) \propto \Phi_a\left(s\right)$. On very long time scales, this relationship is almost surely incorrect with the two fluids interacting in a complicated way.

But to establish a strawman, supposing the proxy temperatures to be proportional to ocean heating, one would infer that on time scales somewhat longer than available in the altimetry, the sea level spectrum should become a bit steeper than white noise,

$\approx s^{-0.3}$, as in $\Phi_a(s)$. The simplest rationalization for the absence of evidence for this behavior is that the altimetric sea level data at periods between about 1 and 15 years are dominated not by thermodynamic processes, but are primarily a mechanical response to wind fluctuations having a near-white frequency spectrum (see e.g., Sturges and Hong, 1995; Frankignoul et al., 1997; Sturges et al., 1998). At much longer periods, presumably the thermodynamic (and freshwater exchange) response would be great enough to emerge from the wind-driven circulation backgrounds.

We here propose a strawman power density spectrum for the oceanic pressure field, one that would approximate also the sea level power density, extending out to the 100ky time scale of the glacial-interglacial shifts of the late Pleistocene. We suggest that at periods of about 100ky and longer that the power density is white noise. The presumption then is that at periods between about 100ky and 50years that the oceanic response is to an approximate buoyancy forcing (manifesting itself both through fresh water injection/-removal and thermal transfers) which is white noise (interpreting the Huybers and Curry result as implying a temperature change with power density of approximately s^{-1}) and producing an oceanic sea level change proportional to s^{-1} as Eq. (6) would suggest.

Between 50 and 15 years, it is supposed that the sea level frequency spectrum is approximately white (as seen in Fig. 12), again forced primarily by atmospheric wind fluctuations. As $s \to 0$, Eq. (3) is constant in s, implying white noise in frequency, and which is accepted as at least not inconsistent with present knowledge. Apart from what is implicit in the frequency-wavenumber spectrum itself, not much is known of the degree to which the small-scale structures do persist into very low frequencies (that is, does the mesoscale have a low-frequency cut-off?). To render the spectral result somewhat less abstract, Fig. 13 displays four, four-year mean, sea surface height anomalies relative to the nine-year mean, 1993-1999, subtracted from the AVISO product (R. Ponte, private communication, 2009). That much small-scale structure persists through four-year averages (and a 16-year one, not shown) suggests that no such mesoscale frequency cut-off exists. These structures are not time-independent "standing-eddies", but temporal anomalies.

The spectral energy must vanish on scales larger than the ocean basins. Beyond that, little is known, although some qualitative inferences can be made from the fragmentary observations of large scale hydrographic variability. A considerable literature has now developed showing "trend-like" behavior in the large-scale hydrographic fields (Roemmich and Wunsch, 1984; Joyce et al., 1999; Arbic and Owens, 2001; Polyakov et al., 2005; Johnson et al., 2007, and many others.) These results are plagued by poorly documented changes in observational technologies and calibrations over time, strong spatial and temporal aliasing, near-surface seasonal biases and, often, the use of unjustified long-distance extrapolations of sparse results. Just as temporally intermittent sampling of noisy data can produce apparent long term trends (see e.g., Wunsch, 2008), sparsely sampled noisy spatial fields can produce spurious large-scale shifts. On the other hand, there is no evidence in the ocean for any sort of spectral gaps, and one *expects* a forced, turbulent, system like the ocean to vary on all time and space scales. Thus large-scale, low-frequency oceanic variability is almost surely present, out to the long-wavelength cutoff at the oceanic basin scale of about 40,000km.

Interpretation of published hydrographic results confronts exactly the same problems of interpretation already encountered in the altimetric/sea level data sets—is one seeing a secular trend or "merely" a long-term red noise fluctuation—hugely exaggerated in difficulty by the comparatively (to the sea level measurements) space and time sampling sparsity? (Bryden et al., 2003, is a rare report of apparently oscillatory behavior in long-term hydrographic data.) To account, formally, for the very long-time, large scale behavior, Eq. (3) is modified to,

$$\Phi(k,s) = \left[1-\exp\left(-D^2k^2\right)\right] B(s,k)\, A(\phi,\lambda) \times \tag{7}$$
$$\left[\operatorname{sech}^4\left(\beta(\phi)\, R_d(\phi,\lambda)^2\, k + s\right)/0.008\exp(-100s^2) + \frac{1}{a_1 + a_4k^4 + \delta_1 s^2}\right],$$
$$D = 8.6\times 10^3\mathrm{km}, \quad s > 0$$

{phiks2}

where the leading factor suppresses the energy as $1/k \rightarrow 40,000$km, and $B(s,k)$ describes the further multiplicative modification of the frequency/wavenumber spectrum in the range $1/40,000\mathrm{km} \leq k \leq 1/20\mathrm{km}$, $0 < \varepsilon_1 \leq s \leq 1/15\mathrm{y}$ and ε_1 is a small, unspecified number introduced to prevent the zero frequency limit from being inferred. Given the difficulties described of interpreting the low-frequency variability, at the present time, B is tentatively written as,

$$B(k,s) = \frac{1}{b_1 + b_2 s},$$

with the constants unspecified. Determining its true form will be a challenging problem. The value of D brings Φ to 95% of its full value when $k = 1/5000$km.

4 The Vertical Structure

Little has been said thus far about the vertical structure of the corresponding pressure fields. This problem is discussed by Wunsch (2009) and FW2010: the major difficulty is that almost everything that is known from observation is based upon the mooring results in Wunsch (1997) and similar studies, and which are spatially scattered and of limited duration and vertical coverage. A very rough inference is that about 50% of the water column kinetic energy lies in the barotropic mode (a bit less in the Pacific, a bit more in the North Atlantic), and 30-40% in the first baroclinic one (modes being the BTT ones defined for a flat bottom and unforced free surface). The remaining kinetic energy lies in higher modes and observational noise. Because the relative contribution of the first baroclinic mode to the *surface* kinetic energy, as seen by an altimeter, is greatly amplified owing to the general increase of the buoyancy frequency towards the surface, it is easy to forget the important role of the barotropic mode in the great bulk of the water column. At periods beyond about a year, there is essentially no information from observations and little prospect for any, without a dedicated observation program—rendering it difficult to test what model results do exist.

The BTT modes used in Wunsch (1997) are a complete set for representing u, v (the solution to a Sturm-Liouville problem), but they would become an inefficient representation for motions confined at or near the sea surface and/or those being forced there by w. Philander (1978) reviews the structure of motions forced at the sea surface and a non-linear generalization has been given under the title "surface quasi-geostrophic (SQG) theory" by e.g., LaCasce and Mahadevan (2006) or Isern-Fontanet et al. (2008); see FW2010. The simplest interpretation of energy in Fig. 5 distant from the flat-bottom modal curves and the non-dispersive line, is that it is a linear response to atmospheric forcing, but a considerable literature would insist that it is the result of turbulent cascades. Presumably all mechanisms are operating to a degree. As far as the mooring data are concerned, no evidence has emerged calling for vertical structures in u, v not effectively described by the first few BTT modes, and so relying on their completeness, SQG and other vertically trapped motions are now ignored. (A surface-trapped mode in the data can be represented perfectly by the linear, flat-bottom modes, with its presence implying a phase-locking (coherence) among them; FW2010 discuss this problem further. Note that there are many moorings showing *bottom* intensification, likely associated with finite topographic slopes; these are not detectable in deep water with the altimeter.) Coupling between the barotropic and first baroclinic modes with a phase amplifying the near-surface kinetic energy will *reduce* the abyssal kinetic energy reminiscent of the Tailleux and McWilliams (2001) topographic energy reduction mechanism. Distinguishing between these two different reasons for mode coupling will not be simple.

In Wunsch (2009), it was speculated that motions along the non-dispersive line represent a phase coupling of the barotropic and first baroclinic modes, but at the moment, the hypothesis has not proved testable. For present purposes, the most agnostic approach is to assert that the energy partition found from the moorings is reasonable, and one might write the full spectrum in the mixed fashion as,

$$\Phi_3\left(k,s,z\right)=\Phi\left(k,s\right)\left[\left(5/10\right)F_0{}^2+\left(4/10\right)F_1\left(z\right)^2+\varepsilon\right] \tag{8}$$

{vertical1}

where F_j are the barotropic and baroclinic modes normalized to unit squared integrals and ε is an error term. The coupling is being ignored as its sign and structure are poorly known. As above, geographical factors are introduced to reflect the spatial variations of Φ, and the vertical partition likely also varies with position. Eq. (8) does permit a zero-order estimate of the depth dependence of the transport variability. (If desired, a formal three-dimensional spectrum can be readily contrived using delta-functions for vertical wavenumbers.)

5 Implications

Trends

The interest in trends primarily concerns those that are truly secular—defined above as extending over far longer intervals than the record length. In many geophysical processes, there is a strong tendency to produce extended periods of *apparent,* but not truly secular, trends (e.g., Wunsch, 1999). The definition of "far longer" is intentionally vague. The reason for being so vague is the suspicion that much of the climate system, having many long time scales, exhibits a conventional memory, red-noise-like, behavior out to extremely long periods.

Real records containing trends can be written,

$$y_t = F(t) + n_t,$$

where $F(t)$ is the trend and is defined here as a process indistinguishable from deterministic. n_t is referred to as "noise" but contains all of the other physics in the record and is regarded as fundamentally stochastic. Here, $F(t)$ will be assumed to generally be linear, $F(t) = a + bt$, but quadratic, cubic, or any other plausible rule can be dealt with similarly (and see Appendix A). Most trends of climate interest have at least a projection onto a straight line.

Sea level provides an interesting example of some of the challenges. From very robust information in the geological record, it is clear that global mean sea level rose during the last deglaciation by about 120m over about 18,000 years (e.g., Bard et al., 1996; Peltier and Fairbanks, 2006) for a gross secular trend of about 0.7 cm/yr. Even this trend is not truly secular as, deeper in the past, it reverses, with global mean sea level dropping as the continental glaciers built up. For present purposes, it is viewed as deterministic, but on much longer time scales, discussions of its nature become bound up with the murky discussion of the controls on the 100,000 year time-scales of the last 800,000 years (see Tziperman et al., 2006 for various references) and it evidently has a mixed stochastic-deterministic character.

The sea level rise curve appears to have flattened considerably during the last about 8000 years (the late Holocene) and one is tempted to compute a new secular trend during this period. Such a computation is surely sensible; the complications arise in the calculation of its statistical significance. As Percival and Rothrock (2005) have noted forcefully, calculation of a trend over an interval chosen visually as a sub-region of a much longer record produces a much more pessimistic confidence interval than does one calculated without the use of a pre-selected interval.

The instrumental sea level records available to us are far shorter than the time scale of the gross shift under deglaciation. High accuracy altimetry exists, as of this writing, for only 16 years. A number of tide gauge records (e.g., Douglas et al., 2001) extend back about 100 years and longer, and the Brest tide gauge record has been patched together back to 1711 by Wöppelmann et al. (2008). These comparatively long records suffer, however, as do altimetric and all other long records, from the inability to fully determine trends introduced by the measurement system. Tide gauge records, depending upon location, undergo major corrections for local tectonic shifts, and often they are relocated at various times in harbors with changing configurations from construction, the technology changes, etc. Even for the modern altimetric data, there are serious concerns about drifts in corrections: Wunsch et al. (2007, Appendix) and Ablain et al. (2009) describe some of the altimetric corrections susceptible to unknown trends.

In addition to sea level and the associated heat and freshwater contributions, the other source of public agitation has been the inference of trends in oceanic volume or mass transports, and (usually only implicitly) the associated enthalpy transports. The physics, and hence the statistics, of transport fluctuations and of sea level change are quite distinct, albeit not independent—with a relationship through the pressure field.

In any region, the statistical significance of a trend-law will be determined in large-part by the spectrum of the background variability. As discussed in textbooks (e.g., Wunsch, 2006, P. 133+), the most straightforward estimate will involve using the space-time covariance, $R(\tau,\rho)$ which, through the generalized Wiener-Khinchin theorem (see Vanmarcke, 1983) is the double Fourier transform of the spectrum,

$$R(\tau,\rho) = \iint_{-\infty}^{\infty} \exp\left(2\pi i s\tau + 2\pi i k\rho\right) \Phi(s,k)\, ds dk. \tag{9}$$

{covar2}

Here τ and ρ are the temporal and spatial separations between two points in a region small enough that Φ is representative of both. A full interpretation of R, and the actual calculation of large-scale trends and their significance would take us far beyond the intended scope of this paper. But as an indicator of how Φ, and hence, R, can be used, Fig. 15 displays the two one-dimensional integrals, $R_\tau(\tau)$, $R_\rho(\rho)$ of $R(\tau,\rho)$ in which the spatial and temporal separations, respectively, have been integrated out. They have been normalized to 1 at the origin so that they are autocorrelations (e.g., R_τ is the conventional temporal autocorrelation at one point.) Thus, integrating over all wavenumbers two measurements at one point will effectively be decorrelated after about 200 days, and two measurements at one time will be spatially decorrelated when separated by about 1000km when accounting for the variability out to 16 years.

When trends are computed over particular areas, one would account for spatial averages by integrating appropriately over $R(\tau,\rho)$ and accounting for the scale factor $A(\theta,\lambda)$. Application in this way is postponed to a later paper.

Other Applications.

Many applications of an analytical spectrum exist. For example Wunsch (2008) calculated the loss of coherence in zonally separated measurements and in Wunsch (2009) discussed the remarkably rapid *meridional* loss of coherence of the transports (which involves the meridional spectral density not dealt with here).

6 Discussion

The problem of trend determination in the ocean circulation motivates an attempt to formulate a useful frequency-wavenumber representation of the background oceanic variability. That goal in turn leads to a long list of physics puzzles. An empirival analytical form is proposed for the zonal-wavenumber and frequency content of surface pressure (elevation) variability in the subtropics. Unlike a previous model of ZW2001, it is heavily asymmetric in the eastward and westward-going phase velocities, with much of the energy lying along the sharply-defined non-dispersive line—whose slope is a function of latitude, approximately βR_d^2. About 20% of the energy is eastward-going. A speculative form of the spectral behavior for periods beyond the current length of the altimetric records (16 years) is proposed.

Within the observed time scales, the proposed analytical form seems typical of subtropical latitudes, but it clearly fails in the Southern Ocean and elsewhere, although these failures are not described here. Because the cut-off frequency for baroclinic Rossby waves rapidly diminishes with β, and hence with latitude, even 15 years of data proves short for discussing high latitude behavior. Theoretical explanations of the frequency structures observed are not readily available, as turbulence (and unequilibrated instability) theories do not normally address the *time-domain* structure seen at mid-latitudes. There is thus a mismatch of observational capability, which finds frequency spectra easiest to estimate, and the theoretical constructs which are simplest in wavenumber or directed at transient behavior.

Several physical theories address rapidly propagating Rossby waves producing narrow-bands in frequency-wavenumber space, and several other theories are directed at turbulent interactions producing broadband characters in that space. No comprehensive theory exists that describes either the numerical or analytical spectral versions in Figs. 5-7, or 10, although various theories predict e.g., breakup of waves into unstable modes, and hence, turbulence (Isachsen et al., 2007), or formation of waves from the turbulence at the Rhines scale, etc. Much of the theoretical uncertainty, only sketched here, could be reduced by better understanding of, (A) the modal partition of the motions and, (B) the degree of phase locking among the modes and which could be better explored with existing data.

The parameter called U, which is supposed to represent alternatively a Taylor-hypothesis large-scale mean advection velocity, or an RMS of the energy containing eddies is best denoted $\tilde{U}$—it will be a *sample* value and itself a stochastic variable. Except in special places like the Antarctic Circumpolar Current, its value and sign would be expected to vary considerably from one-realization of duration T, to another. Discussions of the sampling statistics of U as a function of duration and area do not seem to be available. Whether the sharpness, overall stability, and latitude dependence of the non-dispersive line are consistent with fluctuations in the sampled U, is unknown.

Baroclinic instability will populate the ocean with low mode energy, and turbulent cascade arguments (going back at least to Charney, 1971), will redistribute that energy in both wavenumber and vertical mode space (see e.g., Fu and Flierl, 1980; Vallis, 2006; Scott and Arbic, 2007; and others). Cascades of energy can take place either up- or down-scale in wavenumber, and in transfers e.g., to and from barotropic mode and first and higher baroclinic modes.

What are the implications of these results for determining trends? Mathematically, the behavior of the spectrum in the low frequency limit, $s \to 0$, is crucial because it determines whether the autocovariance decays exponentially, as with conventional random processes, or algebraically as in so-called long memory processes in which the behavior of the spectrum is that of a power law to arbitrarily long time scales. In practice, the limiting case is inaccessible from observation and not likely even physically meaningful. What is accessible are estimates of the spectral behavior for small $s > 0$, limited by record lengths. Because the presence of a trend influences that behavior, the spectral density estimates obtained here are ambiguous—ranging from purely "white" to weakly "red" and dependent upon precisely how the estimate is made. No specific evidence exists for any more exotic behavior involving so-called long memory processes—given the very long, conventional, time scales present in the ocean circulation.

Altimetric data, now of order 16+ years duration show that considerable structure exists in the frequency-wavenumber domain for small s, and that the frequency spectrum $\Phi_s(s)$, obtained by integrating out the wavenumber spectrum, will be a function of (at least) latitude. Thus the statistical signficance of any particular observed trend (a subject not explored here), will depend directly upon the geography and areal extent of the region under consideration. In particular, attaching significance levels to putative global average trends requires integration over the spatially varying structures in the background variability. Treating that background variability as geographically homogeneous can lead to incorrect conclusions about significance.

7 Appendix. Piecewise-Linear Trends

The assumption that the sea level is best represented as a straight line trend plus a stochastic background is not easy to test. As one generalization, the best fit of a minimal number of linear segments produces a useful alternative representation. Here we use the "ℓ_1 trend filtering" method of Kim et al. (2009), which is based upon minimizing the cost function,

$$J = \|\eta(t) - f(t)\|_2 + \alpha^2 \|Df(t)\|_1 , \tag{10}$$

{cost1}

where $f(t)$ is a set of continuous line segments, D is an operator computing the numerical second derivatives, and α^2 is an empirical trade-off parameter. Note that the straight lines fit $\eta(t)$ is a least-squares sense (2-norm), but the numerical second derivatives are measured in a $1-$norm (absolute value) sense. See Kim et al. (2009) for a discussion of the rationale for this choice. Fig. 16 shows the result, for the Honolulu tide gauge record, of choosing the value of α^2 giving the smallest 1-norm for $f(t)$. Whether this result is a more useful one than the simple fit above to the entire record is debatable. That a single, simple, trend does not describe such a complex phenomenon as sea level change is, however, unsurprising. The nature of the estimated low frequency spectrum as $s \to 0$ is sensitive to the number of separate line segments that might be subtracted from records such as this one, or alternatively, as it would be if no trend is subtracted, and the number of pieces treated as though part of the fractionally observed low frequencies.

Acknowledgments. Supported in part by the National Aeronautics and Space Administration through JPL Jason grant NNX08AR33G. I had useful discussions with B. Owens, C. Wortham, and R. Ferrari, and some of the anonymous reviewers' comments led to significant improvements.

References

Ablain, M., A. Cazenave, G. Valladeau, and S. Guinehut, 2009: A new assessment of the error budget of global mean sea level rate estimated by satellite altimetry over 1993-2008. *Ocean Sci.,* 5, 193-201.

Arbic, B. K. and W. B. Owens, 2001: Climatic warming of Atlantic intermediate waters. *J. Clim.,* 14, 4091-4108.

Bard, E., B. Hamelin, M. Arnold, L. Montaggioni, G. Cabioch, G. Faure, and F. Rougerie, 1996: Deglacial sea-level record from Tahiti corals and the timing of global meltwater discharge. *Nature*, 382, 241-244.

Beran, J., 1994: *Statistics for Long Memory Processes.* Chapman and Hall, New York, 315pp.

Bindoff, N. L., J. Willebrand, coordinating lead authors, 2007: Oceanic climate change and sea level. Chapter 5 of *IPCC Fourth Assessment Report. The Physical Science Basis,* Cambridge Un. Press, 387-432.

Bryden, H. L., E. L. McDonagh, and B. A. King, 2003: Changes in ocean water mass properties: Oscillations or trends? *Science,* 300, 2086-2088.

Cazenave, A. and R. S. Nerem, 2004: Present-day sea level change: Observations and causes. *Revs. Geophys.,* 42.

Charney, J. G., 1971: Geostrophic turbulence. *J. Atm. Sci.*, 28, 1087-1095.

Chelton, D. B.and M. G. Schlax: 1996: Global observations of oceanic Rossby waves, *Science,* 272, 234-238.

Chelton, D. B., M. G. Schlax, R. M. Samelson, and R. A. de Szoeke, 2007: Global observations of large oceanic eddies. *Geophys. Res. Letts.*, 34.

Chelton, D. B., R. A. DeSzoeke, M. G. Schlax, K. El Naggar, and N. Siwertz, 1998: Geographical variability of the first baroclinic Rossby radius of deformation. *J. Phys. Oc.*, 28, 433-460.

Colosi, J. A. and W. Munk, 2006: Tales of the venerable Honolulu tide gauge. *J. Phys. Oc.*, 36, 967-996.

Douglas, B. C., Kearney, M. S. and S. R. Leatherman, Eds., 2001: *Sea Level Rise, History and Consequences.* Academic, San Diego, 228.

Ferrari, R. and C. Wunsch, 2009: Ocean circulation kinetic energy: reservoirs, sources, and sinks. *Ann. Rev. Fluid Mech.,* 41, 253-282

Frankignoul, C., P. Muller, and E. Zorita, 1997: A simple model of the decadal response of the ocean to stochastic wind forcing. *J. Phys. Oc.*, 27, 1533-1546.

Frankignoul, C., A. Czaja, and B. L'Heveder, 1998: Air-sea feedback in the North Atlantic and surface boundary conditions for ocean models. *J. Clim.*, 11, 2310-2324.

Fu, L.-L. and A. Cazenave, 2000: *Satellite Altimetry and Earth Sciences : A Handbook of Techniques and Applications.* Academic Press, xii, 463 p. pp.

Fu, L-L and G. R. Flierl, 1980: Non-linear energy and enstrophy transfers in a reaslistically stratified ocean. *Dyn. Atm and Oceans,* 4, 219-246.

Garrett, C. J. R. a. W. H. Munk., 1972: Space-time scales of internal waves. *Geophys. Fl. Dyn., 3,* 225-264.

Glazman, R. E., and P. B. Weichman, 2005: Meridional component of oceanic rossby wave propagation. *Dy. Atm. Oceans*, 38, 173-193.

Hinze, J. O., 1975: *Turbulence.* 2d ed. McGraw-Hill, New York, 790pp.

Huybers, P. and W. Curry, 2006: Links between annual, Milankovitch and continuum temperature variability. *Nature,* 441, 329-332.

Isachsen, P. E., J. H. LaCasce, and J. Pedlosky, 2007: Rossby wave instability and apparent phase speeds in large ocean basins. *J. Phys. Oc.,* 37, 1177-1191.

Isern-Fontanet, J., G. Lapeyre, P. Klein, B. Chapron, and M. W. Hecht, 2008: Three-dimensional reconstruction of oceanic mesoscale currents from surface information. *J. Geophys. Res.*, 113.

Johnson, G. C., S. Mecking, B. M. Sloyan, and S. E. Wijffels, 2007: Recent bottom water warming in the Pacific Ocean. *J. Clim.*, 20, 5365-5375.

Joyce, T. M., R. S. Pickart, and R. C. Millard, 1999: Long-term hydrographic changes at 52 and 66 degrees W in the North Atlantic subtropical gyre & Caribbean. *Deep-Sea Res. I-Topical Studies in Oceanography*, 46, 245-278.

Katz, E. J., 1975: Tow spectra from MODE. *J. Geophys. Res.*, 80, 1163-1167.

Killworth, P. D., and J. R. Blundell, 2003: Long extratropical planetary wave propagation in the presence of slowly varying mean flow and bottom topography. Part I: The local problem. *J. Phys. Oc.*, 33, 784-801.

——, 2003: Long extratropical planetary wave propagation in the presence of slowly varying mean flow and bottom topography. Part II: Ray propagation and comparison with observations. *J. Phys. Oc.*, 33, 802-821.

Kim, S. J., K. Koh, S. Boyd, D. Gorinevsky, 2009: l(1) Trend Filtering. *SIAM Review*, 51, 339-360.

Kutzbach, J. E., 1978: Nature of climate and climatic variations. *IEEE Trans. Geosci. Rem. Sensing,* 16, 23-29.

LaCasce, J. H. and A. Mahadevan, 2006: Estimating subsurface horizontal and vertical velocities from sea-surface temperature. *J. Mar. Res.*, 64, 695-721.

Le Traon, P. Y., F. Nadal, and N. Ducet, 1998: An improved mapping method of multisatellite altimeter data. *J. Atm. Oc. Tech.*, 15, 522-534.

Longuet-Higgins, M. S., 1965: Planetary waves on a rotating sphere. II. *Proc. Roy. Soc., A,* 284, 40-68.

McCoy, E. J., A. T. Walden, and D. B. Percival, 1998: Multitaper spectral estimation of power law processes. *IEEE Transactions on Signal Processing*, 46, 655-668.

Maharaj, A. M., P. Cipollini, N. J. Holbrook, P. D. Killworth, and J. R. Blundell, 2007: An evaluation of the classical and extended rossby wave theories in explaining spectral estimates of the first few baroclinic modes in the south pacific ocean. *Ocean Dyn.*, 57, 173-187.

Maximenko, N. A., O. V. Melnichenko, P. P. Niiler, and H. Sasaki, 2008: Stationary mesoscale jet-like features in the ocean. *Geophys. Res. Letts.,* 35.

Mazloff, M. R., P. Heimbach, C. Wunsch, 2010: An eddy-permitting Southern Ocean state estimate. *J. Phys Oc.,* in press.

Mitchell, J. M., 1976: Overview of Variability and its causal mechanisms *Quat. Res.* 6, 481-493.

Overland, J. E., D. B. Percival, and H. O. Mofjeld, 2006: Regime shifts and red noise in the North Pacific. *Deep-Sea Res.*, 53, 582-588.

Peltier, W. R. and R. G. Fairbanks, 2006: Global glacial ice volume and Last Glacial Maximum duration from an extended Barbados sea level record. *Quat. Sci. Revs.,* 25, 3322-3337.

Percival, D. B. and A. T. Walden, 1993: *Spectral Analysis for Physical Applications : Multitaper and Conventional Univariate Techniques.* Cambridge University Press, xxvii, 583 p. pp.

Percival, D. B. and D. A. Rothrock, 2005: "Eyeballing" trends in climate time series: A cautionary note. *J. Clim.*, 18, 886-891.

Percival, D. B., J. E. Overland, and H. O. Mofjeld, 2001: Interpretation of North Pacific variability as a short- and long-memory process. *J. Clim.*, 14, 4545-4559.

Philander, S. G. H., 1978: Forced oceanic waves. *Revs. Geophys.* 16, 15-46.

Polyakov, I. V., U. S. Bhatt, H. L. Simmons, D. Walsh, J. E. Walsh, and X. Zhang, 2005: Multidecadal variability of North Atlantic temperature and salinity during the twentieth century. *J. Clim.*, 18, 4562-4581.

Rhines, P. B., 1977: The dynamics of unsteady currents. *The Sea*, 6, 189-318.Wiley.

Roemmich, D. and C. Wunsch, 1984: Apparent changes in the climatic state of the deep North Atlantic Ocean. *Nature,* 307, 447-450.

Scott, R. B. and B. K. Arbic, 2007: Spectral energy fluxes in geostrophic turbulence: Implications for ocean energetics. *J. Phys. Oc.*, 37, 673-688.

Smith, R. L., 1993: Long-range Dependence and Global Warming, in *Statistics for the Environment*, eds. V. Barnett and KF Turkman, New York: Wiley, pp. 141-161.

Sturges, W. and B. G. Hong, 1995: Wind forcing of the Atlantic thermocline along 32°N at low-frequencies. *J. Phys. Oc.*, 25, 1706-1715.

Sturges, W., B. G. Hong, and A. J. Clarke, 1998: Decadal wind forcing of the North Atlantic subtropical gyre. *J. Phys. Oc.*, 28, 659-668.

Tailleux, R., and J. C. McWilliams, 2001: The effect of bottom pressure decoupling on the speed of extratropical, baroclinic rossby waves. *J. Phys. Oc.*, 31, 1461-1476.

Tulloch, R., J. Marshall, K. S. Smith, 2009: Interpretation of the propagation of surface altimetric observations in terms of planetary waves and geostrophic turbulence. *J. Geophys. Res.,* 114 Article Number: C02005.

Tziperman, E., M. E. Raymo, P. Huybers, and C. Wunsch, 2006: Consequences of pacing the Pleistocene 100 kyr ice ages by nonlinear phase locking to Milankovitch forcing. *Paleoceanography*, 21

Vallis, G., 2006: *Atmospheric and Oceanic Fluid Dynamics.* Cambridge Un. Press, Cambridge, 745pp.

Vanmarcke, E., 1983: *Random Fields Analysis and Synthesis.* The MIT Press, Cambridge, 382.

Vinogradov, S. V., R. M. Ponte, P. Heimbach, and C. Wunsch, 2008: The mean seasonal cycle in sea level estimated from a data-constrained general circulation model. *J. Geophys. Res.*, 113

Vyushin, D. I., and P. J. Kushner, 2009: Power-law and long-memory characteristics of the atmospheric general circulation.*J. Clim.*, 22, 2890-2904.

Wöppelmann, G., N. Pouvreau, A. Coulomb, B. Simon, and P. L. Woodworth, 2008: Tide gauge datum continuity at Brest since 1711: France's longest sea-level record. *Geophys. Res. Letts.*, 35.

Wunsch, C., 1997: The vertical partition of oceanic horizontal kinetic energy. *J. Phys. Oc.*, 27, 1770-1794.

Wunsch, C., 1999: The interpretation of short climate records, with comments on the North Atlantic and Southern Oscillations. *Bull. Am Met. Soc.,* 80, 245-255.

Wunsch, C., 2006: *Discrete Inverse and State Estimation Problems: With Geophysical Fluid Applications.* Cambridge University Press, xi, 371 p.

Wunsch, C. and P. Heimbach, 2007: Practical global oceanic state estimation. *Physica D*, 230, 197-208.

——, 2008: Mass and volume transport variability in an eddy-filled ocean. *Nature Geosci.,* 1, 165-168.

——, 2009: The oceanic variability spectrum and transport trends. *Atm.-Ocean,* 47, 281-291.

Wunsch, C. and P. Heimbach, 2009: The Global Zonally Integrated Ocean Circulation, 1992-2006: Seasonal and Decadal Variability. *J. Phys. Oc.,* 39, 351-368.

Wunsch, C., R. M. Ponte, and P. Heimbach, 2007: Decadal trends in sea level patterns: 1993-2004. *J. Clim.*, 20, 5889-5911.

Zang, X. Y. and C. Wunsch, 1999: The observed dispersion relationship for North Pacific Rossby wave motions. *J. Phys. Oc.*, 29, 2183-2190.

——, 2001: Spectral description of low-frequency oceanic variability. *J. Phys. Oc.,* 31, 3073-3095.

Figure Captions

1. Region used to study sea level and transport variability. Only the eastern half of the box (east of dashed line) is used for some of the spectral calculations to avoid the very energetic Kuroshio and Kuroshio extension region. The Hawaiian arc, the location of the Honolulu gauge (black dot), is visible just to the south of the box. The box was purposely located to avoid that major topographic interruption.

2. Sea surface anomaly (cms) at weekly intervals showing the degree of variability present. Week 1 starts on 14 October 1992.

3. Logarithm to the base 10 of the sea surface variance (cm^2) showing the great spatial inhomogeneity of the field. This chart is visually little different when the annual cycle is removed.

4. The trend, in m/y in the region. In general the trend is much less than the standard deviation.

5. Normalized frequency/wavenumber spectrum as estimated for the eastern sub-region in Fig. 1 (from Wunsch, 2009) along 27°N. Left panel shows the power linearly, and the right panel is its logarithm. Normalization renders the maximum value as 1, so that only the shape is significant here. Dashed lines show the linear Rossby wave dispersion relationship in the barotropic and first baroclinic modes, with the meridional wavenumber, $l = 0$, and the dash-dot lines assume $l = k$ for unit aspect ratio.

6. Frequency, $\Phi_s(s)$ (left panel), and zonal wavenumber, $\Phi_k(k)$, spectra of η for the eastern part of the study region. Wavenumber spectra are shown as westward-(solid) and eastward- (dashed) going energy. Vertical dash-dot line denotes the annual cycle which is

only a small fraction of the total energy and which (see Fig. 5) is dominated by the lowest wavenumbers, indistinguishable here from $k = 0$. Approximate 95% confidence limits can be estimated as the degree of high frequency or wavenumber variablity about a smooth curve and are quite small. (From Wunsch, 2009). The spectra are normalized so that they are dimensionless cycles/day or cycles/km.

7. The logarithm of the energy density, as in Fig. 5, except at 41°N. Thin white line is the new tangent to the first baroclinic mode at $s = k = 0$, and the dotted white line is the tangent line of Fig. 5. At this higher latitude, the tangent line is much shallower. Notice that the energy lying along the nondispersive line is reduced, with a noticeable corresponding growth near $k = 0$ at all frequencies. Dashed white lines are the linear dispersion curves for the barotropic and first baroclinic modes with $l = 0$.

8. Contours in m/s (upper panel) of the time average zonal flow, u,over 16 years at each point in the latitude-longitude range shown from ECCO-GODAE solution v3.73. Lower panel shows the spatial average velocity over the latitude band of the upper panel, but only the eastern half of the region, along with its spatial standard deviation.

9. Slope of the first baroclinic mode dispersion relationship as $s \to 0$ as a function of position. Evaluated from Chelton et al. (1998). Values are in km/day. The dispersion relationship is modified near the equator, from the equatorial β-plane, and values are not shown.

10. Upper left panel is the same as the logarithmic spectrum in Fig. 5, and the right panel is the suggested analytical form in Eq. (3). Lower panels show the summed out $\Phi_s(s)$, (left), and $\Phi_k(k)$ (right). The values are normalized so that power is dimensionless.

11. Estimate of the *shortest* period (in days) possible in the first baroclinic Rossby wave, computed from βR_1, where R_1 was estimated by Chelton et al. (1998). Values near the equator must be computed from a different dispersion relationship and are not shown here.

12. Upper panel is the monthly-mean 103 year Honolulu tide gauge record (from the Permanent Service for Mean Sea Level, Liverpool), before and after trend removal. (See Colosi and Munk, 2006 for a detailed discussion of this record). Twoe power density spectral estimates are shown in the left panel before trend removal. One estimate is from a Daniell window applied to a periodogram (using 8 frequency bands, solid line), and the second is a multitaper spectral estimate (Percival and Walden, 1993) shown as dotted. Approximate 95% confidence interval is for the latter. A power law of $s^{-1.1}$ is a best fit to the multitaper estimate in the frequency band corresponding to periods between about 500 and 55 days. At the lowest frequencies, removal of the trends (right panel) shifts the spectral shape from weakly-red to nearly white.

13. Four-year time average of the AVISO altimetric product relative to the nine-year mean surface. That small scale structures are observed even after four years of averaging suggests that the mesoscale can exist at all frequencies. (Courtesy of R. Ponte.) Note that the anomalies are relative to a nine-year mean subtracted by the AVISO group, and not coincident with the entire record length.

14. Coherence amplitude as a function of frequency and zonal separation for the analytical power density spectrum.

15. Left and right panels are respectively the temporal, $R_\tau(\tau)/R_\tau(0)$, and $R_\rho(\rho)/R_\rho(0)$, autocorrelations derived from the analytical frequency wavenumber spectral density.

16. Piecewise linear fit (in a 2-norm) to the two-year running mean Honolulu tide gauge record such that the 1-norm of the straightlines is a minimum as shown in Fig. **??** {1}

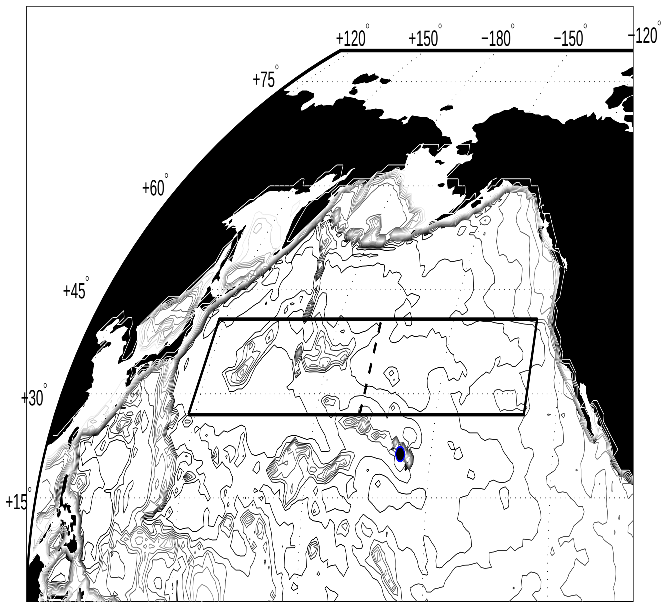

Figure 1: Region used to study sea level and transport variability. Only the eastern half of the box (east of dashed line) is used for some of the spectral calculations to avoid the very energetic Kuroshio and Kuroshio extension region. The Hawaiian arc, the location of the Honolulu gauge (black dot), is visible just to the south of the box. The box was purposely located to avoid that major topographic interruption.

{globalpositi

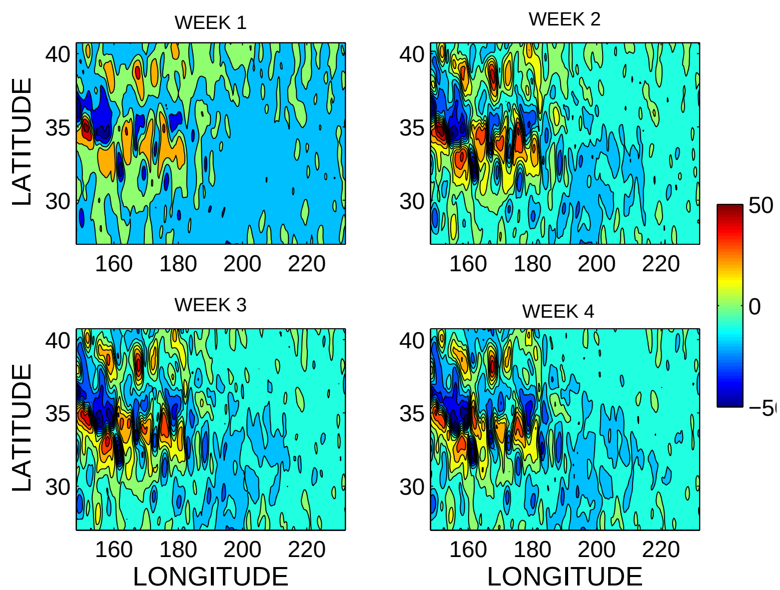

Figure 2: Sea surface anomaly (cms) at weekly intervals showing the degree of variability present. Week 1 starts on 14 October 1992.

{snapshots.ep

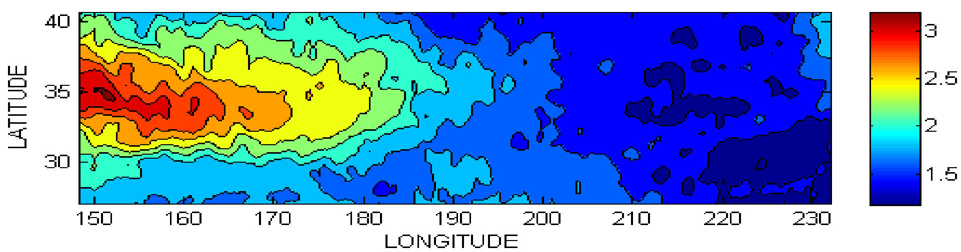

Figure 3: Logarithm to the base 10 of the sea surface variance (cm^2) showing the great spatial inhomogeneity of the field. This chart is visually little different when the annual cycle is removed.

{variancechar

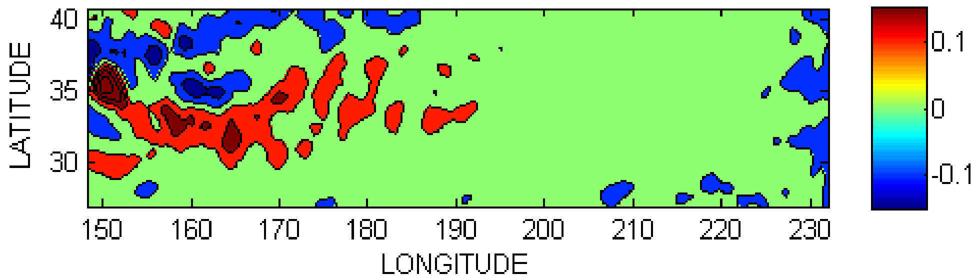

Figure 4: The trend, in m/y in the region. In general the trend is much less than the standard

{trend.tif}

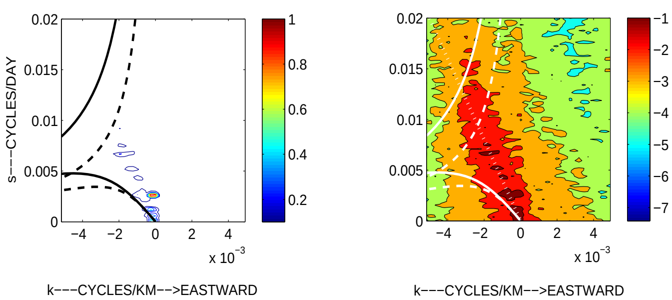

Figure 5: Normalized frequency/wavenumber spectrum as estimated for the eastern sub-region in Fig. 1 (from Wunsch, 2009) along 27°N. Left panel shows the power linearly, and the right panel is its logarithm. Normalization renders the maximum value as 1, so that only the shape is significant here. Dashed lines show the linear Rossby wave dispersion relationship in the barotropic and first baroclinic modes, with the meridional wavenumber, $l = 0$, and the dash-dot lines assume $l = k$ for unit aspect ratio.

{region1_east

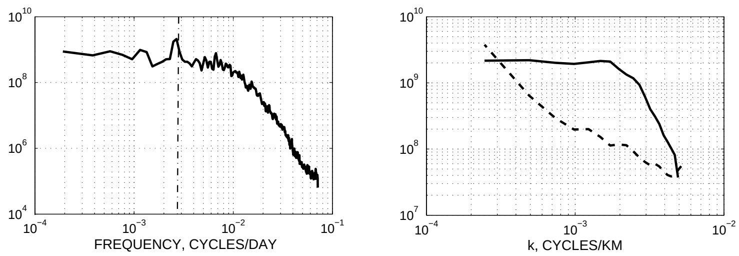

Figure 6: Frequency, $\Phi_s(s)$ (left panel), and zonal wavenumber, $\Phi_k(k)$, spectra of η for the eastern part of the study region. Wavenumber spectra are shown as westward-(solid) and eastward- (dashed) going energy. Vertical dash-dot line denotes the annual cycle which is only a small fraction of the total energy and which (see Fig. 5) is dominated by the lowest wavenumbers, indistinguishable here from $k = 0$. Approximate 95% confidence limits can be estimated as the degree of high frequency or wavenumber variablity about a smooth curve and are quite small. (From Wunsch, 2009). The spectra are normalized so that they are dimensionless cycles/day or cycles/km.

{one_dspectra

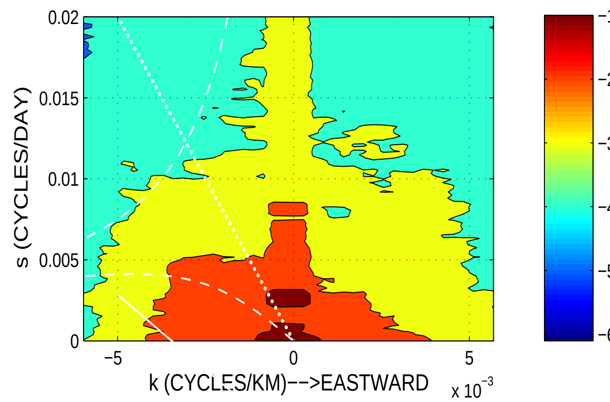

Figure 7: The logarithm of the energy density, as in Fig. 5, except at 41°N. Thin white line is the new tangent to the first baroclinic mode at $s = k = 0$, and the dotted white line is the tangent line of Fig. 5. At this higher latitude, the tangent line is much shallower. Notice that the energy lying along the nondispersive line is reduced, with a noticeable corresponding growth near $k = 0$ at all frequencies. Dashed white lines are the linear dispersion curves for the barotropic and first baroclinic modes with $l = 0$.

{region1_east

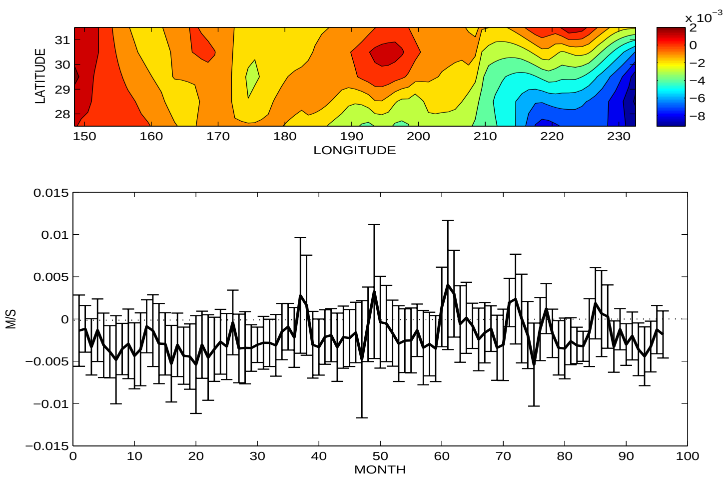

Figure 8: Contours in m/s (upper panel) of the time average zonal flow, u,over 16 years at each point in the latitude-longitude range shown from ECCO-GODAE solution v3.73. Lower panel shows the spatial average velocity over the latitude band of the upper panel, but only the eastern half of the region, along with its spatial standard deviation.

{timemeancont

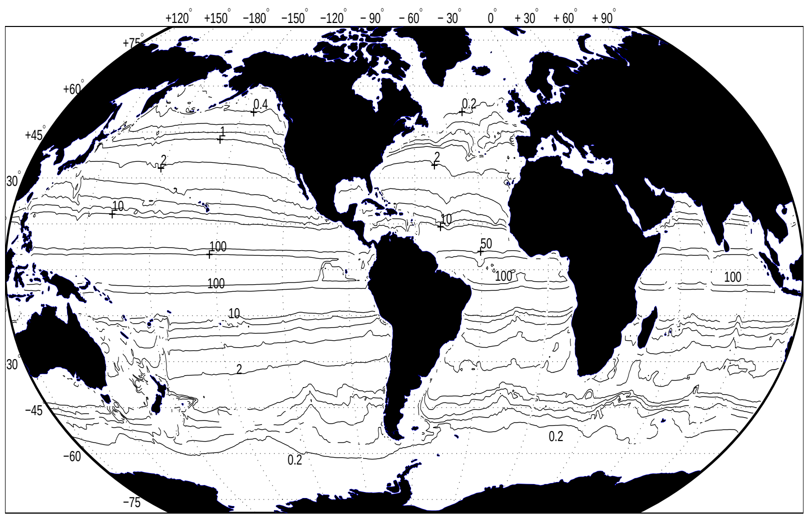

Figure 9: Slope of the first baroclinic mode dispersion relationship as $s \to 0$ as a function of position. Evaluated from Chelton et al. (1998). Values are in km/day. The dispersion relationship is modified near the equator, from the equatorial β-plane, and values are not shown.

{dispersion_s

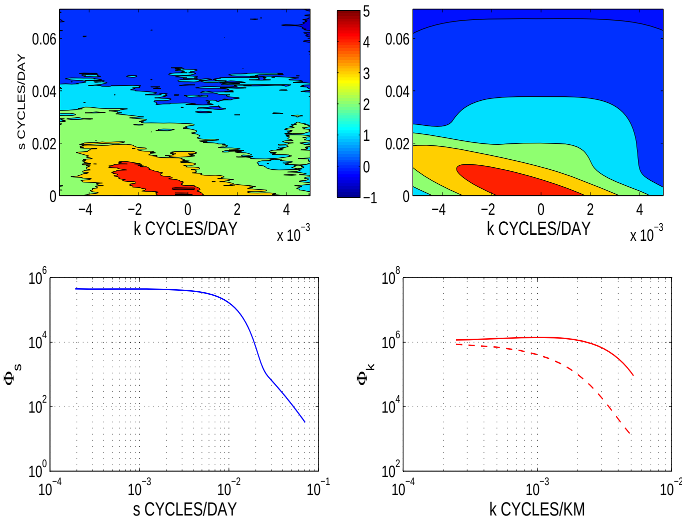

Figure 10: Upper left panel is the same as the logarithmic spectrum in Fig. 5, and the right panel is the suggested analytical form in Eq. (3). Lower panels show the summed out $\Phi_s(s)$, (left), and $\Phi_k(k)$ (right). The values are normalized so that power is dimensionless. {analytic_pd_

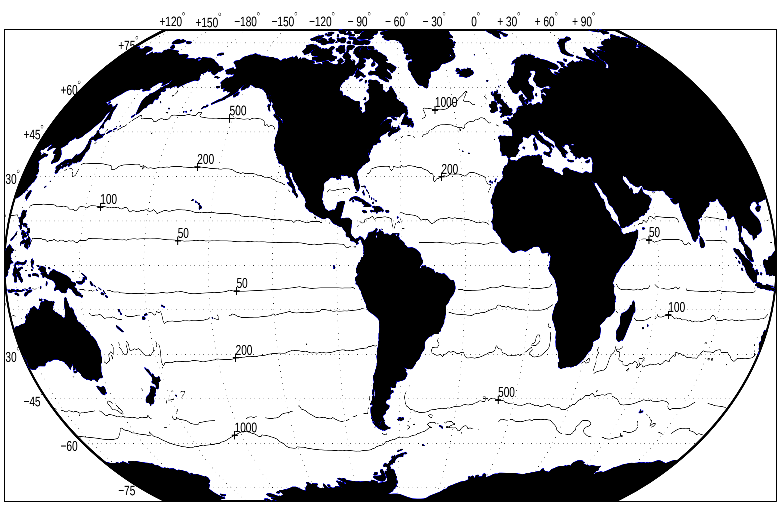

Figure 11: Estimate of the *shortest* period (in days) possible in the first baroclinic Rossby wave, computed from βR_1, where R_1 was estimated by Chelton et al. (1998). Values near the equator must be computed from a different dispersion relationship and are not shown here. {cutoff_perio

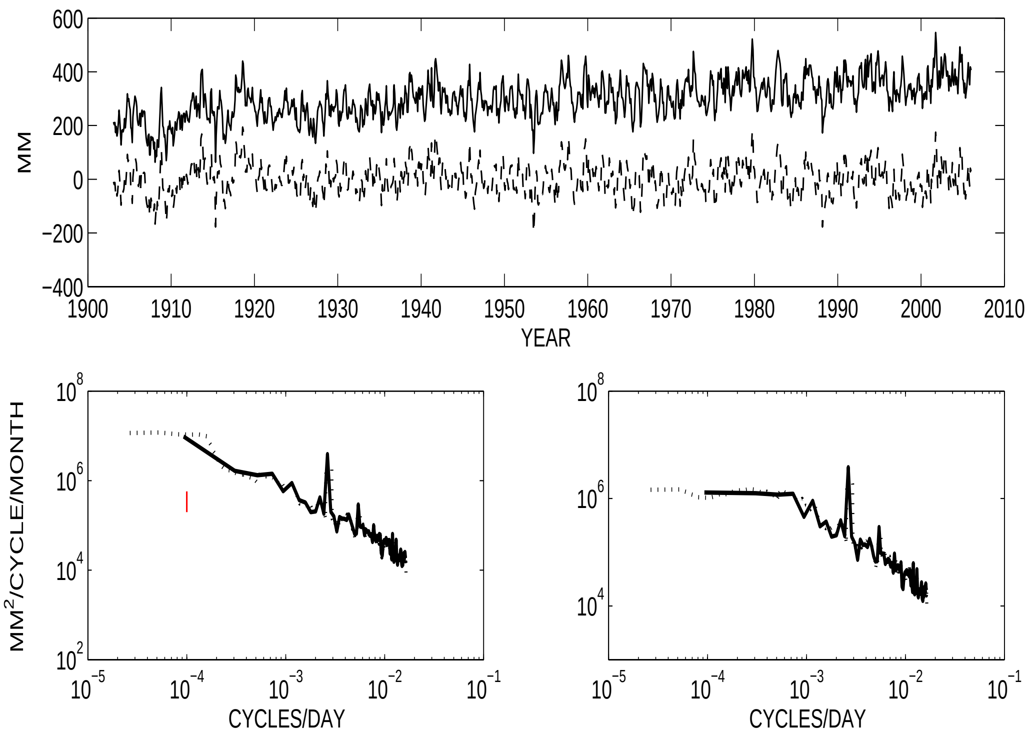

Figure 12: Upper panel is the monthly-mean 103 year Honolulu tide gauge record (from the Permanent Service for Mean Sea Level, Liverpool), before and after trend removal. (See Colosi and Munk, 2006 for a detailed discussion of this record). Twoe power density spectral estimates are shown in the left panel before trend removal. One estimate is from a Daniell window applied to a periodogram (using 8 frequency bands, solid line), and the second is a multitaper spectral estimate (Percival and Walden, 1993) shown as dotted. Approximate 95% confidence interval is for the latter. A power law of $s^{-1.1}$ is a best fit to the multitaper estimate in the frequency band corresponding to periods between about 500 and 55 days. At the lowest frequencies, removal of the trends (right panel) shifts the spectral shape from weakly-red to nearly white.

{hono_pd_2way

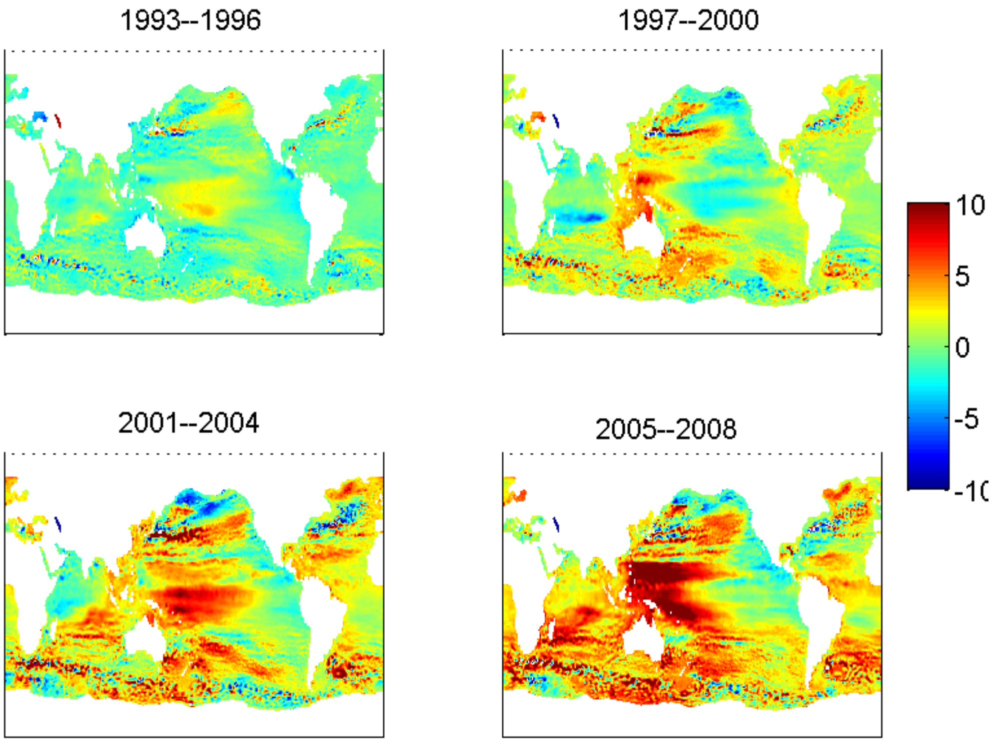

Figure 13: Four-year time average of the AVISO altimetric product relative to the nine-year mean surface. That small scale structures are observed even after four years of averaging suggests that the mesoscale can exist at all frequencies. (Courtesy of R. Ponte.) Note that the anomalies are relative to a nine-year mean subtracted by the AVISO group, and not coincident with the entire record length.

{plot4carl_cw

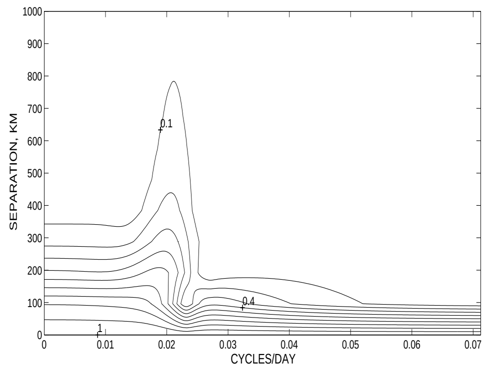

Figure 14: Coherence amplitude as a function of frequency and zonal separation for the analytical power density spectrum.

{coher_analyt

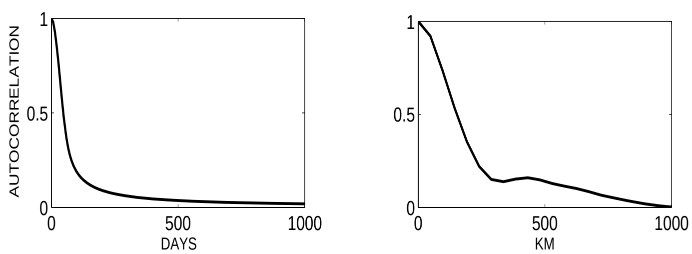

Figure 15: Left and right panels are respectively the temporal, $R_\tau\left(\tau\right)/R_\tau\left(0\right)$, and $R_\rho\left(\rho\right)/R_\rho\left(0\right)$, autocorrelations derived from the analytical frequency wavenumber spectral density.

{autcorrs_ana

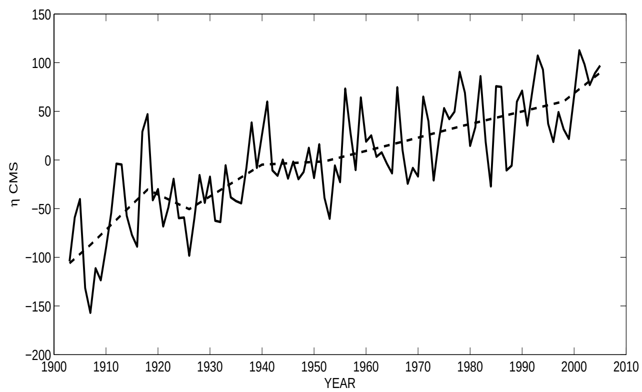

Figure 16: Piecewise linear fit (in a 2-norm) to the two-year running mean Honolulu tide gauge record such that the 1-norm of the straightlines is a minimum as shown in Fig. ?? {honolulu_lin